Implementation and Performance Assessment of Biomedical Image Compression and Reconstruction Algorithms for Telemedicine Applications

Chapter · January 2019

DOI: 10.4018/978-1-5225-7952-6.ch003

4 authors:

Charu Bhardwaj
Jaypee University of Information Technology

Urvashi Sharma
Jaypee University of Information Technology

Shruti Jain
Jaypee University of Information Technology

Meenakshi Sood
National Institute of Technical Teachers Training and Research chandigarh

Medical Data Security for Bioengineers

Butta Singh
Guru Nanak Dev University, India

Barjinder Singh Saini
Dr. B. R. Ambedkar National Institute of Technology, India

Dilbag Singh
Dr. B. R. Ambedkar National Institute of Technology, India

Anukul Pandey
Dumka Engineering College, India

A volume in the Advances in Bioinformatics and
Biomedical Engineering (ABBE) Book Series

IGI Global
DISSEMINATOR OF KNOWLEDGE

Published in the United States of America by
IGI Global
Medical Information Science Reference (an imprint of IGI Global)
701 E. Chocolate Avenue
Hershey PA, USA 17033
Tel: 717-533-8845
Fax: 717-533-8661
E-mail: cust@igi-global.com
Web site: http://www.igi-global.com

Library of Congress Cataloging-in-Publication Data

Names: Singh, Butta, 1981- editor. | Saini, Barjinder Singh, 1970- editor. | Singh, Dilbag, editor. | Pandey, Anukul, editor.
Title: Medical data security for bioengineers / Butta Singh, Barjinder Singh Saini, Dilbag Singh, and Anukul Pandey, editors.
Description: Hershey, PA : Medical Information Science Reference, [2019] | Includes bibliographical references.
Identifiers: LCCN 2018041395| ISBN 9781522579526 (hardcover) | ISBN 9781522579533 (ebook)
Subjects: | MESH: Computer Security | Medical Informatics | Confidentiality | Signal Processing, Computer-Assisted | Cloud Computing
Classification: LCC R858 | NLM W 26.5 | DDC 610.285--dc23 LC record available at https://lccn.loc.gov/2018041395

This book is published in the IGI Global book series Advances in Bioinformatics and Biomedical Engineering (ABBE) (ISSN: 2327-7033; eISSN: 2327-7041)

British Cataloguing in Publication Data
A Cataloguing in Publication record for this book is available from the British Library.

Chapter 3

Implementation and Performance Assessment of Biomedical Image Compression and Reconstruction Algorithms for Telemedicine Applications:

Compressive Sensing for Biomedical Images

Charu Bhardwaj
Jaypee University of Information Technology, India

Shruti Jain
Jaypee University of Information Technology, India

Urvashi Sharma
Jaypee University of Information Technology, India

Meenakshi Sood
Jaypee University of Information Technology, India

ABSTRACT

Compression serves as a significant feature for efficient storage and transmission of medical, satellite, and natural images. Transmission speed is a key challenge in transmitting a large amount of data especially for magnetic resonance imaging and computed tomography scan images. Compressive sensing is an optimization-based option to acquire sparse signal using sub-Nyquist criteria exploiting only the signal of interest. This chapter explores compressive sensing for correct sensing, acquisition, and reconstruction of clinical images. In this chapter, distinctive overall performance metrics like peak signal to noise ratio, root mean square error, structural similarity index, compression ratio, etc. are assessed for medical image evaluation by utilizing best three reconstruction algorithms: basic pursuit, least square, and orthogonal matching pursuit. Basic pursuit establishes a well-renowned reconstruction method among the examined recovery techniques. At distinct measurement samples, on increasing the number of measurement samples, PSNR increases significantly and RMSE decreases.

DOI: 10.4018/978-1-5225-7952-6.ch003

INTRODUCTION

With the advancement in information and communication technology, data traffic generates noticeably massive amount of information data especially in biomedical area. Radiological medical imaging methods (MRI and CT-Scan experiments) are used to inspect and analyze the inner structure of human body. These methods generate a large amount of scientific information which is digitally stored in the form of medical image that can be easily accessible. Clinical imaging records are significantly high as a typical hospital generates terabytes of information per year (Ravishankar & Breler, 2011). Clinical imaging data is certainly excessive and needs more storage space thus medical image compression is essential. Compression is a proficient solution for illustrating compact and robust data representation to facilitate efficient transmission and storage. File size is reduced, less bandwidth is utilized and the transmission speed is accelerated using compression techniques. Predominant goal of compression is to lessen the redundant and irrelevant bits of data for efficient data storage and transmission. Compression may be extensively categorised into two classes, Lossy and Lossless Compression. Lossy compression is appropriate for the applications where a slight loss of information is permissible like for natural pictures, text images, etc. For lossy compression techniques, compression ratio is high but the image quality is low. In case of lossless compression, the reconstructed image is the exact replica of the actual image as there is no data loss in lossless compression technique. Compression ratio achieved for this approach is not always high but the recovered image is of better-quality as compared to that of the lossy compression approach.

Data loss is not tolerable in scientific field like biomedical image processing as it can lead to wrong diagnosis. Many hospitals have small clinics situated in the far flung regions where distance is a vital issue to deliver the health care facilities. Patient residing in remote, rural and semi-urban areas find tough time to travel to far away hospitals particularly for diagnostic functions. For the convenience of patients suffering from severe diseases, the hospitals make use of telemedicine practices to provide health care facilitates in such areas. These tele-radiology applications allow the technician at the remote centres to capture a series of medical image data (MRI or CT scan) and transmit it to the principal health centre situated at the city where the diagnostic radiologist can examine the image and send back the diagnostic information to the clinical prognosis and the patients (Vijaykuymar, & Anuja, 2012).

In conventional image capturing systems, sampling is primarily based on Nyquist criteria wherein the original signal is sampled at a rate more than or equal to two times the maximum frequency of the signal. This sampling rate is too high for certain applications thereby increasing the complications in terms of complexity during compression. The increased rate of sampling adds directly to the complexity of the sensing hardware and this leads to wastage of power resources (Zhao, *et al*., 2017; Wiegand, *et al*., 2003). So, to facilitate the need of image compression for contemporary applications it is required to have a system with decreased acquisition complexity and flexible process for decoding. Compressive Sensing (CS) technique emerges as a new idea for signal acquisition, compression and reconstruction which has become main focus of researcher's interest. It is a far unique technique employing sub-Nyquist sampling criteria overcoming the drawbacks of the conventional strategies (Donoho, 2006; Candes, *et al*., 2008; Romberg, *et al*., 2006). CS utilizes the sparse signal recovery using fewer linear measurements and convex optimization approach for approximate recovery relative to standard schemes utilizing the complete ensemble of signal space (Candes & Romberg, 2007).

The concept of CS was at first introduced by Emmanuel Candes, collectively with Justin Romberg and Terry Tao (Donoho, 2006; Candes, *et al*., 2008; Romberg, *et al*., 2006; Candes, *et al*., 2007). Signals fulfilling the requirement of sparsity in any domain can be recovered using CS approach, may it be an audio, image or a video signal. In (Nahar & Kolte, 2014) it was seen that CS was a progressive approach for signal acquisition and restoration. The key advantages of CS are faster data acquisition from very few sparse samples, reduced computational complexity, low power transmission, small traffic extent, etc. X. Zhang, *et al.* have used Orthogonal Matching Pursuit (OMP) reconstruction algorithm in (Zhang, Wen, Han, & Villasenor, 2011) applying the set of rules to recover an image. It was found that OMP has negligible additional complexity however enabling overall performance improvement in the reconstruction. Combined sparsifying transforms were used in (Qu, Cuo, Guo, Hu, & Chen, 2010) to achieve CS for MRI imaging by enforcing the sparsity of image using Total Variation (TV), wavelet approach, etc. It was seen that smooth L_0 norm method have NP hard problem which was then replaced by Basic Pursuit (L_1) norm minimization. Predefined information was used in (Liang & Ying, 2010) for CS reconstruction that utilises partially known spatial and temporal frequency domains from motion patterns of MR images. Reconstruction was done using L_1 norm minimization technique which was the best approach for image sample recovery. A real time MRI recovery technique was proposed in (Majumdar, Ward, & Aboulnasr, 2012) and the residual (the difference image between the previous and the current image) was taken. M.M Sevak, *et al.* (Sevak, Thakkar, Kher, & Modi, 2012) have implemented wavelet transform for the generation of a set of sparse components and CS approach for compression and later they combined the two techniques. Various Non- Linear Mapping Techniques are compared with OMP technique in (Zhang & Wen, 2012). As compared to the other convex optimization approaches, OMP was less complex approach providing faster running speed, lower power consumption and optimal reconstruction. Guaranteed reconstruction was however provided by convex optimization based recovery algorithms. Scan time for MR image acquisition was improved by T.D.Tran *et al.* (Tran, Duc, & Bui, 2010). In this paper authors combines CS approach along with the wireless transmission mechanism which was based on 802.11 providing bit rate requirement at 11Mbps. An improvised L_1 norm reconstruction method for CS-MRI was proposed in (Chang & Ji, 2010) investigating the previously developed approaches like SMASH and SENSE recovery algorithms. A better recovery algorithm; L_1 norm minimization approach was used in this paper to provide precise details, sharp edges and accurate recovery for MRI image reconstruction. This approach yields lower Normalised Mean Square Error (NMSE) producing a better quality recovered image with less computation complexity. A new set of parameters consisting of different auxiliary measurements, low pass filter coefficients, ordering index, etc. are proposed in (Lakshminarayana & Sarvagya, 2016) for improving the performance of CS algorithm. Authors (Lakshminarayana & Sarvagya, 2016) show that L_1 reconstruction approach was used to recover the signal using the concept of sparsity. A better performance was achieved maintaining the trade-off between compression ratio and medical image quality as compared to the existing literature in this field. Some of the other state of the art literatures are summarized in Table 1.

The main motivation of this chapter is reduction in file size using CS approach for biomedical image compression so as to minimize the storage and bandwidth requirements. The main goal of this chapter is to find an efficient method for reconstruction of images and evaluate recovery algorithms to maintain the balance between image quality and compression ratio. A modified approach for better acquisition, compression and reconstruction using CS technique provides better reconstruction and least distorted compressed image.

Table 1. Literature review of CS techniques

S. No.	Authors	Utilized Techniques	Implication Drawn and Estimated Parameters	Demerits
1.	(Shiqian M., *et.al.*, 2008)	L_1- norm minimization, Total Variation approach and Wavelets	Error of image and Signal-to-Noise-Ratio	Requirement of better image quality and storage space.
2.	(Nagesh P., Baoxin L., 2009)	Compressed sensing Technique (CS)	Recognition rate and percentage of storage space	Multiple views of scenes are used.
3.	(Wright J., *et.al.*, 2009)	L_1- minimization technique for sparse representation	Sparsity Concentration Index (SCI)	Detection of object is also required.
4.	(Sen P., Darabi S., 2011)	Compressive rendering for finding pixel values	MSE is evaluated. Scheme gives better quality reconstruction.	Sampling densities employed are very less.
5.	(Jing C., Wang Y., & Hanxiao W., 2012)	Real time video surveillance CS tracking and motion detection algorithm	Better recovery at high resolution for fast tracking utilizing less storage space.	Outcomes are not evaluated on benchmark datasets.
6.	(Hemalatha R., *et.al.*, 2013)	BinDCT and Noiselet based CS approach is utilized for Energy consumption analysis	Compression ratio, PSNR and reduced bit rate	More energy consumption reduction is required.
7.	(Yipeng L., *et.al.*, 2013)	Biomedical signal recovery using L_1-Total Variation approach and Nuclear norm minimization	Technique employed provide accurate signal recovery and Mean L_1 error is evaluated	Outcomes are not evaluated on benchmark datasets.
8.	(Tremoulheac B., *et.al.*, 2014)	L1 norm minimization with Fourier transform in temporal direction and Alternating Direction Methods of Multipliers (ADMM)	Normalized MSE for intensity and motion	Method is not optimized and run-time elapsed is more.
9.	(Xie S., Guan C., & Lu Z., 2015)	ADMM with variable splitting strategy	MSE is calculated	Datasets are not standardized and approach is computationally complex
10.	(Zhang Q., *et.al.*, 2016)	CS theory is applied from down-sampled l-space data and a wavelet tree-based recovery algorithm is proposed	SNR is calculated for MR images	Can be extended for recovery of dynamic MR sequences
11.	(Bilala M., *et.al.*, 2017)	L1 norm approximations are employed	SSIM, Gaussian noise level in MR images, RMSE of recovered MR images	Complex architecture
12.	(Shrividya G. & Bharathi S.H., 2018)	CS-MRI technique is used along with Total Variation algorithm	MSE, PSNR, SSIM and Sampling percentage of MR images	SSIM value can be improved more to get quality

COMPRESSIVE SENSING

CS plays a significant role in numerous fields like biomedical, scientific imaging and satellite imaging to reconstruct the signal using fewer samples (Foucart, *et al*., 2013; Madhukumar, *et al*., 2015). CS techniques produces better results in terms of high imaging speed, high Compression Ratio (CR) and better quality image (Wang, Bresler, & Ntziachristos, 2011). This technique exploits the samples of sparse signal of interest rather than collecting the entire ensemble of signal samples (Baraniuk, 2007). CS approach intend to acquire sensing and compression in a single step by converting the sensing paradigm (Madhukumar & Baiju, 2015). Figure 1 shows the block diagram of CS technique which is the combination of sensing and compression.

Figure 1. Block diagram of Compressive sensing

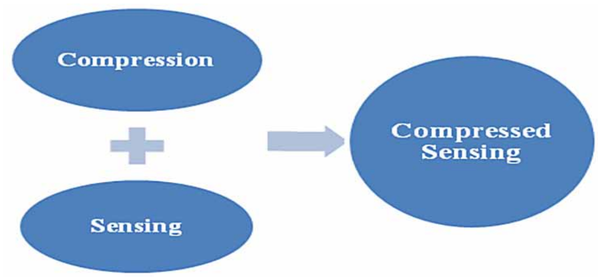

Sensing and Sampling

Sensors are used to sample and analyse the signal by taking a linear measurement of signal space. The whole ensemble of this signal space is not exploited for CS recovery but the CS technique works on alternating present vectors using already known vector space. This sampling consists of measurement samples having decreased dimensions than the original signal. Let the highest frequency component f (in hertz) is maximum for an analog signal then according to Nyquist, the sampling criteria should be at least $2 \times f_{max}$, or twice the highest frequency component. If the sampling criteria is not fulfilled or if the sampling rate is less than the twice of maximum frequency component then highest frequency components does not provide the correct representation of an analog input signal.

The sub-Nyquist sampling has involved a lot of concentration in both fields of mathematics and computer science. Sub-Nyquist sampling, also known as compressed sensing refers to the problem of recovering the signal by its samples. It can also recover the signal from the fewer samples than required by Nyquist sampling criteria. Recovery principles involved in Compressed Sensing approach to recover the signals are briefed in the next section.

Principles of Compressive Sensing Reconstruction

The two recovery principles involved in CS recovery are Sparsity and Incoherence. To implement CS theory, signal of interest is represented by sparsity and an isometric property of incoherence which limits the sensing modality.

Sparsity

Sparsity expresses an idea, that a continuous time signal has the rate of information much lower than expressed by the signal bandwidth. Similarly for a discrete signal to be sparse, the degree of freedom should be much lower than the finite length of the signal. Sparse signals have many zero coefficients and few non-zero coefficients. Fewer non-zero coefficients consist of majority of signal information and the other coefficients are not exactly zero however having very less value. Signal estimation for a sparse signal is done by considering only the larger coefficients consisting of majority information and other least significant coefficients are ignored during computation (Park & Wakin, 2009). A signal can be sparse or compressible having a concise representation in a proper sparsifying (Ψ) basis. Thresholding algorithms also depend on sparsity to estimate the signal. For systems of linear equations, sparse approximation theory deals with sparse solutions. Several variations for sparse approximation problem are structured sparsity and collaborative sparse coding.

1. **Structured Sparsity:** In the original version of sparsity, any of the coefficients of the problem domain can be selected but in case of structured sparsity model, group of coefficients are chosen instead of picking individual coefficients (Eldar, Kuppinger, & Bolcskei, 2010).
2. **Collaborative or Joint Sparse Coding:** Original version of the problem is defined only for single signal but in collaborative sparse coding a set of signal is available and each of them is converged from the same set of coefficients (Tropp, Gilbert, & Strauss, 2006).

Incoherence

The duality between time and frequency domain is expressed by incoherence which basically presents the idea that the signal having sparse representation in sparsifying domain (Ψ) and must be spread out in the sampling domain in which they are acquired. Incoherence for sparse signals is implemented through isometric property. Coherence basically evaluates the maximum correlation between any two elements of entirely two different matrices. Incoherence refers to the property which signifies that there must be minimum correlation between the elements of two different matrices. Considering two different domains, a signal is considered to be compressible if it has high sparsity in Ψ domain and is incoherent in sampling domain (Baig, Lai, & Punchihewa, 2012). Low correlation enables the signal reconstruction of sparse signal with few samples whereas it is impossible for high correlation samples regardless of signal sparsity.

Imaging Modality

A particular imaging technique or a system in the area of Computed Tomography Scan (CT-Scan), nuclear medicine, ultrasound, projection radiography and Magnetic Resonance Imaging (MRI) is termed as imaging modality. Modalities like CT-Scan, projection radiography and nuclear medicine make use of ionization to visualize the interior human body structure. High frequency sound signals are fired into the human body for ultrasound imaging and the echoes are received from the structures within the body. High strength magnetic field and radio waves are combined to acquire MRI images and it exploits the property of nuclear magnetic resonance. The main tool used in biomedical imaging field for acquiring the interior structure of human body is MRI. Notable visualization of human body and its contrast mechanism is employed to obtain the body structure using MRI scan (Ravishankar & Breler, 2011). MRI is different from CT-Scan as this process does not use radiations and CT-Scan uses ionizing radiations which can harm the human body. MRI provides the detailed view of human body which is not indicated in X-Ray, CT-Scan or ultrasound images. Magnetic resonance imaging approach provides better contrasted image and clear diagnostic quality than other imaging modalities like X-Ray and CT- Scans.

MRI Scan

MRI imaging utilizes magnetic resonance scanners exhibiting the properties of Nuclear Magnetic Resonance (NMR). The nucleus of the hydrogen atom tends to align itself in the presence of strong magnetic field. As the vast numbers of hydrogen atoms are present in the human body, it leads to net magnetization of the human body structure. Selective excitation of different regions within the body is also possible by inclining the group of these magnets away from the magnetic field direction. General categories of MR-Scanners are functional MRI (*f*MRI) and Magnetic Resonance Spectroscopic Imaging.

1. **Functional MRI (fMRI):** This scanner, images the blood oxygenation of the human brain by using oxygenation sensitive pulse sequence. fMRI employing an advance MRI in such a way that blood flow is increased to activate regions of brain. Standard MRI-Scanners do not actually detect blood flow as fMRI.
2. **Magnetic Resonance Spectroscopic Imaging:** It is termed as a non-invasive imaging technique as it gives spectroscopic information along with the image. Besides imaging the hydrogen atom, other nuclei are used for magnetic resonance spectroscopic imaging. This can be used to infer the cellular activity information from the human body. Different MRI scan images (leg, foot and brain) are shown in Figure 2.

CT-Scan

CT-Scans make use of X-Rays which are collimated (restricted in their geometrical spread) to travel in a 2D 'fan-beam' approximation. Tissues in the 2D cross-section of the human body create the X-Ray beam which is detected by a number of small detectors. The projections of X-Ray beam are collected from varying angular orientations of the detectors and the X-Ray tube as they rotate around a stationary subject (patient). Different CT-Scan modalities are helical CT and multi-slice CT which are currently being used for 3D imaging.

1. **Helical CT:** This CT-Scan modality is named as helical CT because the X-Ray tube slices out a helix. The detectors and the X-Ray tubes rotate around a circle and the patient is also continuously moving through the circle's center. It can acquire 3D Scan of the whole body very rapidly (in less than a minute).

Figure 2. Different MRI images (a) Leg MRI, (b) Foot MRI, (c) Brain MRI

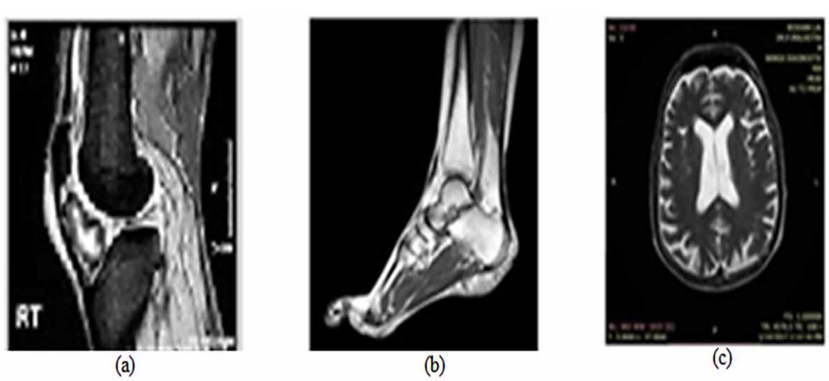

2. **Multi-Slice CT:** It consists of several rows of detectors to speedily gather a cone of X-Ray data which comprises of 2D projection of patients. The quick rotation of X-Ray source and the detectors helps to produce 3D images using CT-Scanners. The different types (leg, foot and brain) of CT scan images are shown in Figure 3.

Compressive Sensing for Medical Images

Biomedical technology is progressing and clinics need to store huge volume of medical data in the form of images and signals to diagnose the current condition of the patients. A standard 12 bit X-ray of size 2048×2560 pixels interpreting 10,485,760 bytes of file size is very huge (ME, et al., 2012). Storage and transmission problem of higher quantity of data can get a breakthrough if the biomedical images are compressed in such a way that not only better quality image is obtained but also less transmission time is required without utilizing high bandwidth.

CS shows the considerable development in the field of biomedical engineering. As an improved framework for sampling and recovery, it is implemented on sparse signal of interest (Liu, Liang, Liu, & Zhang, 2012). In widespread mechanism, radiological images are captured from coupled devices which differentiate it from other information capturing mechanism. Because of presence of external artifacts, massive quantity of noisy data is also present within the informative data which is not required for diagnostic process. As the data is subjected to compression, medical information is compressed along with the undesirable noisy data, but in case of CS, only the desired information is decomposed (Wang, et al., 2011). Medical images like MRI and CT scan takes a long scanning time and these scans are indicative of patient's coronary heart rate, breathing pattern and position which may change time to time leading to degraded diagnosis quality. CS might also reduce poor effects of heart rate variation, pattern of respiration and also reduces the imaging time providing appreciated involvement in medical imaging field (Sevak, *et al*., 2012).

After applying CS for compression the original medical image is also needed to be recovered and its quality is to be assessed so that these images can be utilized for diagnosis purpose. For this reason different recovery algorithms are implemented and their performance is assessed based on image quality parameters and compression ratio.

Figure 3. Different CT-scan images (a) Leg_CT Scan, (b) Foot_CT Scan and (c) Brain_CT Scan

Recovery Algorithms

For optimal reconstruction of signal certain key requirement which should be satisfied are stability, speed, uniform guaranteed reconstruction and efficient performance. Convex optimization technique has gained the popularity due to its better efficiency, highly accurate reconstruction and guarantees the successful reconstruction (Liu, De Vos, Gligorijevic, Matic, Li, & Van Huffel, 2013). Numerous reconstruction strategies are available in the literature and they are detailed below.

Minimum L0 Norm Reconstruction

The exact solution of linear equations for minimum L_0 norm minimization is guaranteed by defining a set of rules. For a signal which is sparse in spasifying domain, the precise recovery is possible by using 2*m* random measurements. Every combination in *m*-sparse vector space is checked to find the exact solution in an N- dimensional space to satisfy the linear system of equations. This reconstruction technique is complex to implement and leads to NP-hard problem (Satyan, 2013).

$$\min \|x\|_0 \text{ subject to } y = \Phi \times x \tag{1}$$

here *x* is the original signal, y is the measurement vector which is obtained by multiplying measurement matrix Φ with the original signal *x*.

Basic Pursuit (L1 Minimization)

It is a convex optimization technique which is also termed L_1 minimization and it provides guaranteed recovery over sparse domain. L_1 minimization technique is not a speedy technique as massive numbers of iterations are involved in this method but it provides robustness for approximating the sparse signal. This technique is not optimally rapid but conversely it is a favourable approach as it gives better quality of reconstruction (Bhatt & Bamniya, 2015). As per the definition of the norm, L_1-norm of signal *x* is defined as,

$$\|x\|_1 = \sum_i |x_i| \tag{2}$$

L2 Norm Minimization

L_2 norm minimization reconstruction algorithm finds the minimum energy solution for minimizing the system of equations. This approach is easier to implement as compared to any other recovery algorithm but the solution provided by this approach is not accurate. Pseudo inverse is calculated to find the solution of L_2 norm but the calculated solution is far away than the optimally correct solution producing the undesired aliasing effect (Candes, *et al*., 2006; Blumensath, *et al*., 2009). L_2-norm is also well known as Euclidean norm, which is used to measure a vector difference and its equation is given by,

$$\|x\|_2 = \sqrt{\sum_i x_i^2} \tag{3}$$

Minimum Total Variation Reconstruction

Total Variation (TV) minimization is a modification in L1 minimization technique that is especially successful in case of imaging applications. It is considered that the image is sparse in its gradient and therefore the image has very few variations in intensity.

$$\min \|s\|_{TV}\text{, subject to } \|\Phi s - y\|_2 \leq \epsilon \tag{4}$$

Eq. (4) defines the TV-minimization reconstruction approach for recovering the gradient sparse signal and here s denotes the transform vector containing k non-zero coefficients, Φ is the measurement matrix, y is the measurement vector and ϵ denotes the upper bound of tolerance for reconstruction error energy (Candes, et al., 2006).

Greedy Method

Compressive sample matching pursuit, orthogonal matching pursuit and stage-wise orthogonal matching, etc. falls into the category of greedy algorithms. Greedy technique presents more rapid reconstruction than simple basic pursuit method but delivers least recoverable sparsity as compared to other reconstruction algorithms like L1 norm minimization. Greedy pursuit often provides uniform guarantee and stability but on the cost of quality. One of the most commonly used greedy algorithms for the recovery of nearly sparse signal is Orthogonal Matching Pursuit (OMP). For each of the new iteration, OMP works iteratively by initially choosing a column with the maximum projection onto the residual signal and then adding it to the already chosen columns. Once choosing a replacement column vector, representation coefficients with respect to the column vectors are chosen and observed through the least square optimization method. This method is not optimally stable but is a speedy reconstruction algorithm as compared to the other recovery approaches (Tropp, 2004).

For performance assessment of these recovery algorithms on medical images, various evaluation parameters are used and they are detailed in the next section.

Performance Evaluation Parameters

There are various performance assessment parameters. In this chapter we are using Mean Square Error (MSE), Peak Signal to Noise Ratio (PSNR), Compression Ratio (CR) and Structural Similarity Index (SSIM) for evaluation of CS recovery algorithms. PSNR is an image quality parameter calculated using MSE and these are inversely related to each other. Higher PSNR value indicates the higher quality of image. SSIM is based on arithmetical values of image and it is based on mean and variance and its value lies in between 0 to 1. The recovered image is structurally similar to the original image if its value leads toward 1. Ratio of compressed bits to the original image bits gives CR of an image (Bhardwaj, *et al.*, 2017; Ji, *et al.*, 2017).

Compressive Sensing: Scope and Its Applications

This section briefs about the various fields and applications where CS technique can be optimally used.

Biomedical Imaging

The technique of creating a visual perception or representation of internal body organs or tissues for medical evaluation and clinical intervention is referred as biomedical imaging. Clinical imaging seeks to reveal the inner body system detailing the pores, skin and bones which are used to diagnose and deal with the diseased body parts. Medical imaging additionally establishes a database of ordinary anatomy and body structure to make it viable to discover abnormalities. Thus better image compression is needed for screening and better diagnosis for biomedical imaging.

Telemedicine

Telemedicine practices allow the clinical services to be used from a distance by the means of modern telecommunication and information technology facilities. Electronic medical information is transferred over a distance to the main diagnostic centre where the information is processed and diagnosed.

Patients residing in the rural areas can take the benefit of medical care facilities without visiting the far away situated hospitals and this helps in removing the distance barriers. Therefore better image compression is required to serve this purpose of telemedicine facility without using much bandwidth and transmission time providing prompt clinical healthcare services.

Multimedia

Multimedia makes use of a combination of variety of contents like audio, video, images, text, animations, etc to make the multimedia applications more interactive. It is different from normal media applications, which makes use of basic conventional computer display like text-only, printed or hand-written material. Multimedia can be recorded, played, displayed, interacted with or accessed via facts content material processing gadgets, which includes automatic and digitally computerized gadgets, but also can be used as a part of live performances. Subsequently arising the need for better image compression to facilitate the multimedia applications to provide an ease to access various facilities.

Virtual Imaging or Digital Photography

An arrangement of electronic photo-detectors is used to capture images in virtual imaging or digital photography. This electronic photo detector is focused by a lens and is exposed on a photographic film to capture a digital photograph. The captured Images are digitized and stored as a computer file equipped with further digital processing, viewing, virtual publishing or printing equipments. Thus there is a need for higher image compression to aid virtual photography.

ALGORITHMS AND IMPLEMENTATION

In this chapter, CS technique is proposed for efficient compression, storage and transmission of MRI and CT-scan medical images. Dataset of MRI and CT-scan benchmark images is acquired from www.physionet.org to test the effectiveness of CS algorithm. For better image recovery different reconstruction algorithms are used and a comparative analysis is done. The following section gives a brief overview of CS algorithm and different recovery algorithms. Implementation and critical performance validation is also done in this section.

CS Algorithm

For the implementation of CS algorithm, consider an input image (x) of dimensions $n \times 1$ and a randomly generated measurement matrix (Φ) of dimensions $m \times n$. If Φ matrix is generated randomly, some useful information might become disoriented so Gaussian distribution is used for random variable generation having mean (μ) as 0 and variance (σ) as 1. Later x and Φ are multiplied to obtain the compressed sized measurement vector y having dimensions $m \times 1$. Steps followed for CS reconstruction are depicted in Figure 4.

Measurement vector y represents the CS sampling procedure and is computed by multiplying the measurement matrix Φ with the original image x.

$$y= \Phi \times x \tag{5}$$

The two main conditions which must be satisfied to recover an image using CS theory are illustrated below. Sampling process structure of CS matrices is depicted in Figure 5 and Figure 6 shows the complete arrangement of CS matrices.

Figure 4. Different steps for Compressive Sensing reconstruction

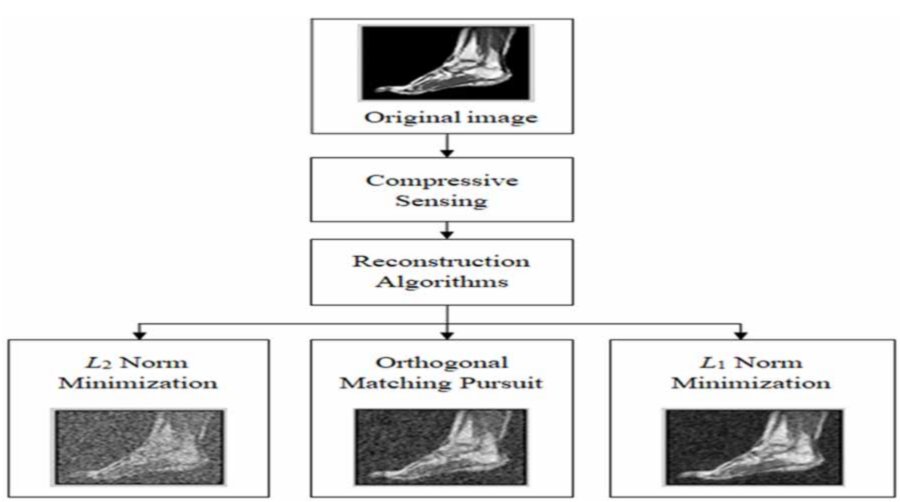

First Condition: Input image (x) should be sparse in some domain for the accurate image reconstruction utilizing few samples. For accurate recovery of an original image, x should fulfil the condition of sparsity i.e., it should be sparse in some domain. Let us consider a sparsifying matrix domain Ψ with dimensions (n× n) and a transform vector s having k significant non-zero coefficients (k<<n). The equation of sparisty is given by,

$$x=\Psi\times s \tag{6}$$

where, Ψ is the sparsifying matrix (n× n) and s is the transform vector containing k non-zero coefficients and k<<n.

Second Condition: The isometric property of incoherence should be satisfied by measurement matrix (Φ) and sparsifying matrix (Ψ) for CS recovery. Signal is more compressible if Ψ is incoherent to Φ and it is stated by the isometric property of incoherence [27]. Incoherence enables a sparse signal to be recovered using less number of samples. The condition of incoherence is denoted by θ in Eq. (7).

$$\theta = \Phi\times\Psi \tag{7}$$

The overall process of sampling is represented by θ' and it becomes,

$$\theta' = \Phi\times\Psi\times s \tag{8}$$

here, Φ is the measurement matrix, Ψ is sparsifying marix and s is transform vector.

Signal recovery for CS technique is achieved using minimization norm equation. By solving the Eq. (9), *x* can be recovered using sparse transform vector *s*,

$$x = \min\left\|\Psi^{-1}\times s\right\|_p \tag{9}$$

where, *Ψ* is sparsifying matrix, *s* is the sparse transform vector and *p* is the signal sparsity.

Figure 5. Sampling process structure of CS matrices

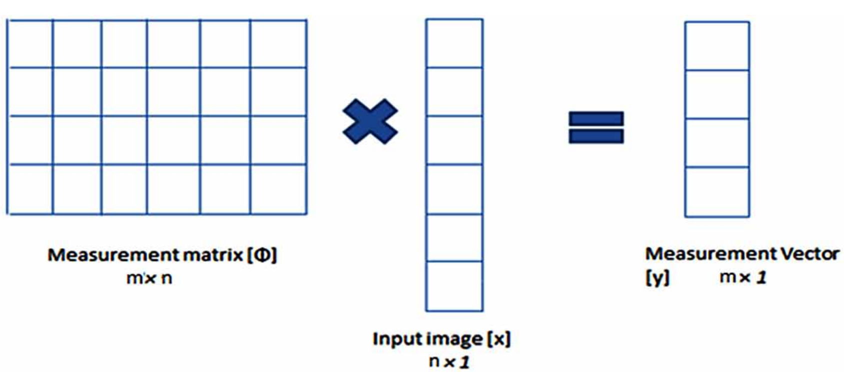

Figure 6. Complete arrangement of CS matrices

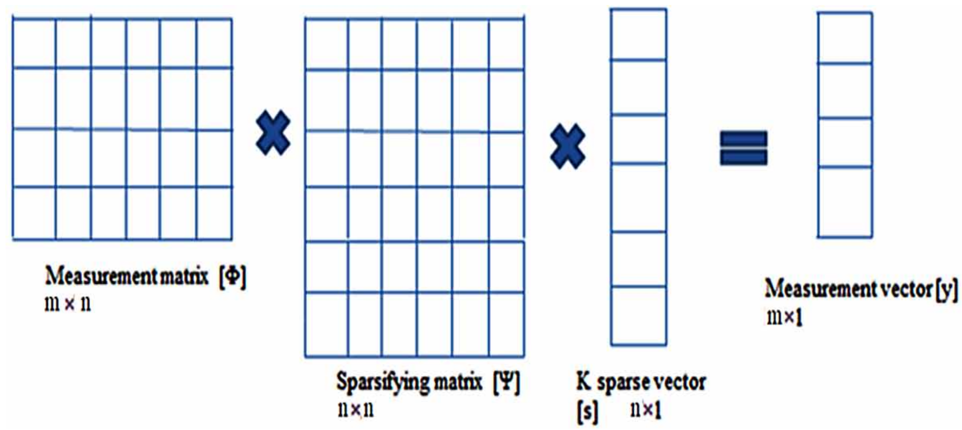

The above equation is reduced to L_0 norm minimization if $p=0$ but it leads to NP hard problem. To resolve this problem, L_1 norm minimization technique is used for reconstruction.

Before analyzing two dimensional (2D) signals, CS is applied on one dimensional (1D) signal to validate the CS algorithm. Consider a 1D signal generated on MATLAB 2013. CS technique is applied on 1D signal having total number of samples (n) = 256 and number of peaks (P) = 6 are considered in the original signal. Keeping n and P constant, measurement samples (m) are varied to recover the original signal using fewer samples than the total number of samples ($m<<n$). Measurement Samples (m) are varied from 16 to 64 to analyze the accurate reconstruction and maintain a trade-off between the sampling rate and accuracy recovery.

Waveforms of 1D signal when CS recovery is applied are shown in Figure 7 to Figure 9 for measurement samples of 16, 32 and 64 respectively. In Figure 7 to Figure 9, x-axis denotes number of samples and y-axis denotes the amplitude of the signal. Three subplots in Figure 7 to Figure 9 represents the original signal, measurement samples considered and recovered signal respectively.

Signal reconstruction for varying number of measurement samples m is shown in Figure7 to Figure 9. It can be seen from Figure 7 that signal is reconstructed with visible distortions if m is considered as 16. On increasing the number of samples, accurate recovery is observed for m as 32 which can be seen in Figure 8. For the value of m ranging from 32 to 64, signal recovery is same as that of original signal. For better signal recover, m should be adjusted in such a way that there is balance between signal quality and sampling rate.

After analysis of CS technique on 1D signal it is applied on medical image samples (2D signal) and the images are recovered using three reconstruction algorithms (L_2 norm minimization, OMP technique and L_1 norm minimization). A detailed discussion of different reconstruction algorithms along with the results obtained are illustrated in the following sections.

CS Recovery Using Least Square Method (L2 Norm Minimization)

The commonly used method to solve the equation ($y = \Phi x$) and to find the minimum energy solution is L_2 norm minimization. The main advantage of this scheme is its simple implementation but it has a drawback that it does not provide the accurate solution producing the image with "aliasing-effect" [32,

Figure 7. Waveforms for m=16

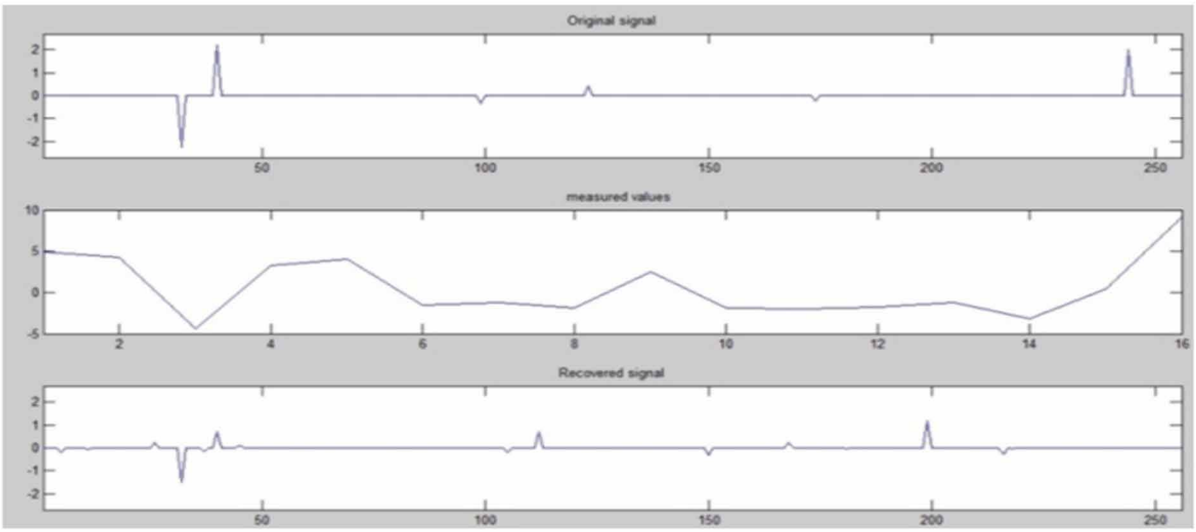

Figure 8. Waveforms for m=32

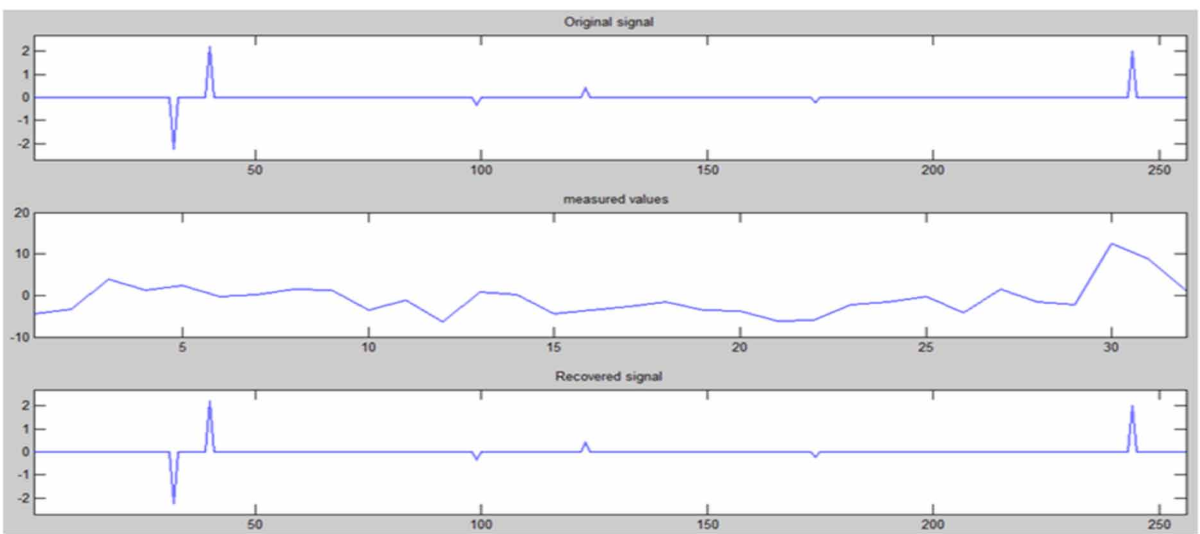

33]. This norm method works on the pseudo inverse based principle. L_2 norm minimization steps are detailed below;

1. Consider $y = \Phi x$ as the system of underdetermined linear equation where y is the measurement vector, x is the original signal, Φ is measurement matrix and $\Phi \in R^{m \times n}$ here ($m<n$).
2. One particular solution for L_2 norm is given by the following equation ;

Figure 9. Waveforms for m=64

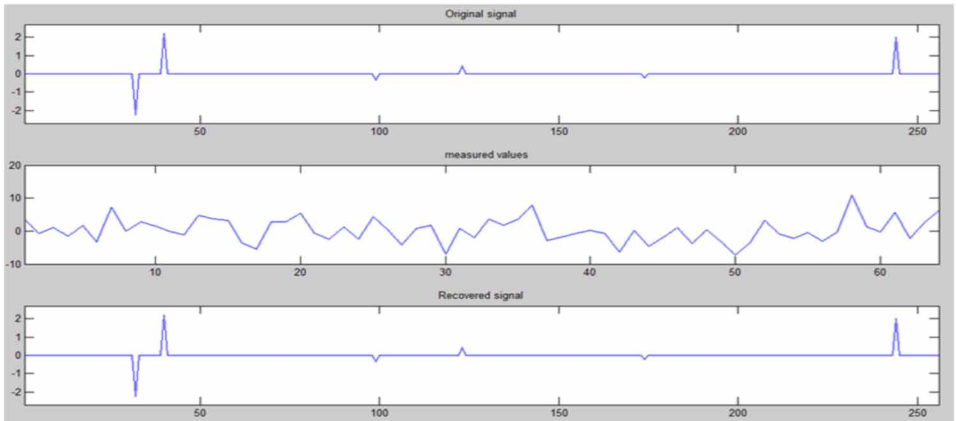

$$\tilde{x} = \Phi^T \left(\Phi\Phi^T\right)^{-1} \tag{10}$$

here $\Phi\Phi^T$ is invertible since Φ is a full rank matrix.

$\breve{x}$ is the solution of $y = \Phi \times x$ that minimizes x and provides the solution of optimization problem.

Figure 10 (a) depicts the original foot MRI image and Figure 10 (b) depicts the reconstructed image obtained using Least Square method (L_2 norm minimization). Figure 10 (c) and Figure 10 (d) shows the respective histograms of original and reconstructed images respectively. In the Figure 10 (a), (b) and Figure 11 (a), (b) x axis and y axis shows horizontal and vertical dimensions of the image. Figure 10 (c), (d) and Figure 11 (c), (d) x axis shows dynamic range of grey scale ranging from 0 to 255 and y axis represents intensity value. Similarly, the original foot CT-Scan image and recovered image using L_2 norm minimization is depicted in Figure 11 (a) and Figure 11 (b) respectively. Figure 11 (c) and Figure 11 (d) shows histograms of original and reconstructed CT-Scan image respectively. It is clear from the

Figure 10. (a) Original image of foot MRI-scan, (b) reconstructed image obtained from Least Square (L_2) and (c) histogram of original image and (d) histogram of reconstructed image

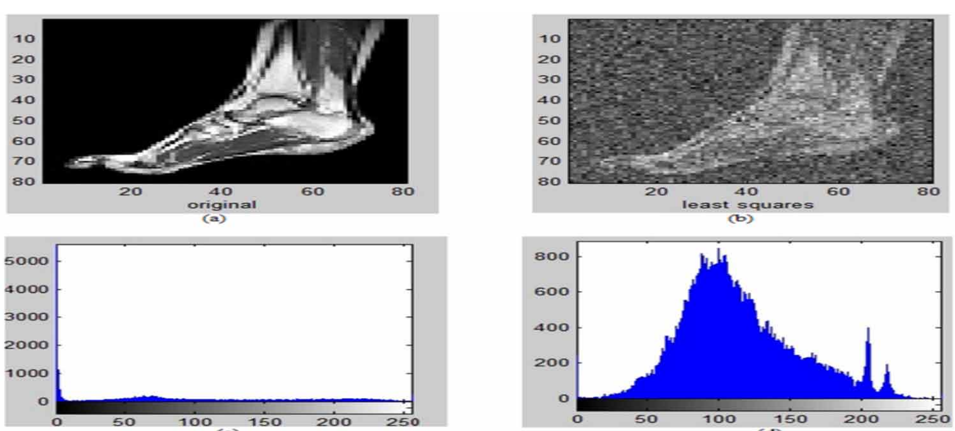

Figure 11. (a) Original image of foot CT-scan, (b) reconstructed image obtained from Least Square (L_2) and (c) histogram of original image and (d) histogram of reconstructed image

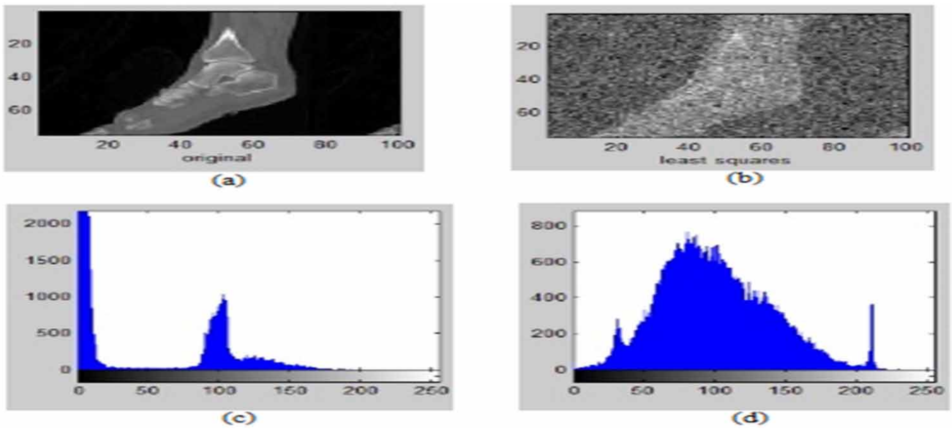

visual representation that the image recovered by L_2 norm minimization is not of better quality and this is further validated after calculating different performance assessment parameters obtained in Table 2. For evaluation purpose we have used 5 images of MRI and 5 images of CT-Scan.

RMSE calculated for L_2 reconstruction method gives a high RMSE value which in turn provides a lower value of PSNR in dB indicating poor image quality. SSIM index is human vision perception based structural similarity index and its value for L_2 norm method is more near 0 indicating less structural similarity to that of the original image.

CS Recovery Using Orthogonal Matching Pursuit (OMP)

Algorithms of matching pursuit like CS Matching Pursuit, Regularization Orthogonal Matching Pursuit and stage-wise Orthogonal Matching Pursuit all falls into the category of greedy algorithms. An estimated signal is obtained by finding the correlation between the columns of Φ measurement matrix and

Table 2. Different performance parameters obtained for L_2 recovery algorithm

Image Samples	RMSE	PSNR (dB)	SSIM
Img1_MR	55.82	12.62	0.43
Img2_MR	52.15	13.33	0.27
Img3_MR	89.79	10.89	0.20
Img4_MR	50.69	13.23	0.44
Img5_MR	46.33	14.65	0.31
Img1_CT	81.16	9.75	0.19
Img2_CT	43.60	14.40	0.21
Img3_CT	39.33	15.91	0.17
Img4_CT	90.12	8.87	0.20
Img5_CT	93.27	7.08	0.17

the measurement residual (r). The new estimated signal (x_k) is highly correlated with the residual [34, 35]. The steps of OMP algorithm are detailed as follows;

1. First of all the residual is initialize, $r_0 = y$ and Column C_0 is set as Φ for iteration count $k=1$.
2. Column vector Φ_{ck} of Φ is obtained using approximation a_c i.e., highly correlated with the residual and the equation is given by;

$$\Phi_{ck} = \max_c \left|\left\langle r_{k-1}, a_c \right\rangle\right|, c \in \left[n\right] \tag{11}$$

3. Least square problem is solved by:

$$x_k = \left\| y - \Phi_{ck} \times x \right\|_2 \tag{12}$$

4. To remove the contribution of a_c (approximation), the residual is updated by

$$r_k = y - \Phi_{ck} \tag{13}$$

5. Increase the iteration count k, and repeat steps 2-4 until stopping criterion is met.

Figure 12 (a) depicts the original foot MRI image and Figure 12 (b) depicts the reconstructed image obtained using Matching Pursuit method (OMP). Similarly, the original foot CT-Scan image and recovered image using OMP is depicted in Figure 13 (a) and Figure 13 (b) respectively. It is clear from the visual representation that the image recovered by OMP reconstruction method gives better recovered image as compared to the L_2 norm minimization and this is further validated after calculating different performance assessment parameters for OMP reconstruction algorithm obtained in Table 3.

Figure 12. (a) Original image of foot MRI-Scan, (b) reconstructed image obtained from Matching Pursuit (OMP) and (c) histogram of original image and (d) histogram of reconstructed image

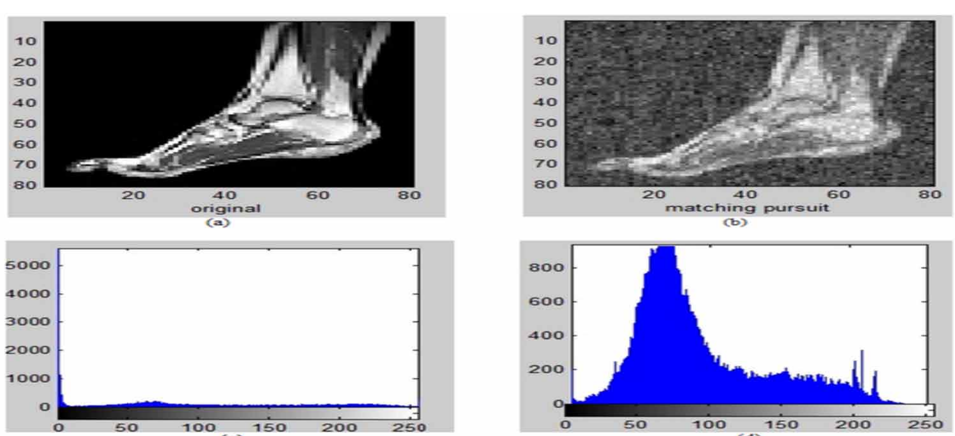

Figure 13. (a) Original image of foot CT-Scan, (b) reconstructed image obtained from Matching Pursuit (OMP) and (c) histogram of original image and (d) histogram of reconstructed image

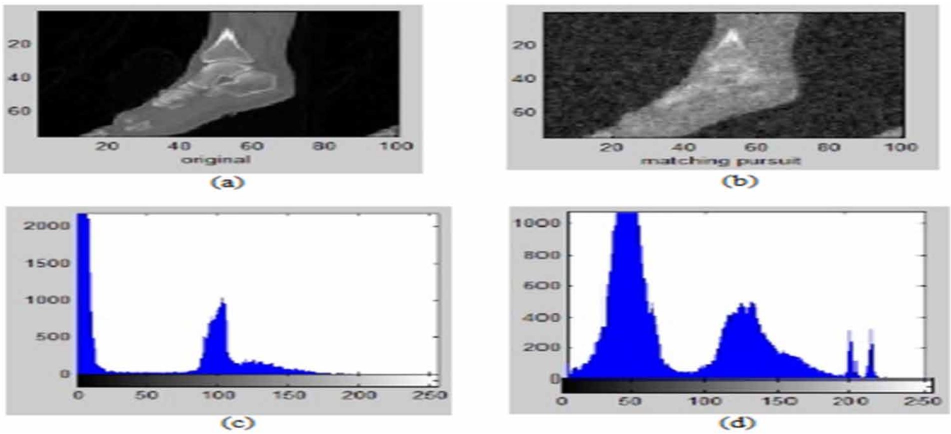

Table 3. Different performance parameters obtained for OMP recovery algorithm

Image Samples	RMSE	PSNR (dB)	SSIM
Img1_MR	39.19	15.84	0.51
Img2_MR	30.16	18.00	0.53
Img3_MR	41.32	15.42	0.49
Img4_MR	36.32	16.48	0.64
Img5_MR	31.26	17.53	0.46
Img1_CT	31.01	17.13	0.48
Img2_CT	14.39	22.32	0.51
Img3_CT	15.31	26.71	0.40
Img4_CT	37.74	16.17	0.44
Img5_CT	53.45	13.26	0.49

RMSE calculated for OMP was less than L_2 reconstruction method thus OMP recovery method provides greater value of PSNR in dB indicating better image quality. Structural similarity index is also near to 0.5 which shows that the recovered image is 50% similar to that of the original medical image. Image recovered using OMP reconstruction method gives better results as compared to L_2 norm minimization method in terms of image quality indicative by image pixel values and also in terms of visual perception based similarity parameter.

CS Recovery Using Basic Pursuit (L1 Norm Minimization)

The best established reconstruction technique is Re-weighted L_1 norm minimization that is used for CS image recovery in contrary to the other reconstruction technique. Uniform guaranteed recovery and stability is provided by L_1 norm minimization approach [32]. There is no linear bound on run time for this technique and it provides better recovery but it is optimally slow. On solving the following minimization problem, x is recovered by solving the equation,

$$x = \min \left\| \Psi^{-1} \times s \right\|_p \tag{14}$$

where, Ψ is sparsifying matrix, x is the original signal and p is the signal sparsity.

L_1 norm minimization recovery steps are as follows:

1. Weight (w) is initially given by $w_i^{(0)} = 1$, for $i = 1\ldots N$. $w_i^{(0)}$ is the weights on pixels, the iterative count is set to 0.
2. By using equation (12), the weighted L_1 minimization problem is solved.

$$\min \left\| W \times s \right\|_1 \text{, s.t., } y = \Phi \times x \tag{15}$$

where W_s are the total number of weights in transform domain s.

3. Weights are then updated for i=1… N,

$$w_i^{(j+1)} = \frac{1}{\left| \tilde{s}_i^{(j)} \right| + \in} \tag{16}$$

Here, s is the sparse transform vector. ϵ is a positive number and use to prevent zero-valued denominator and j refers to number of iterations.

4. After that a specific maximum number of iteration $j_{\max}$ is attained by j and convergence terminates; otherwise increase j and repeat step 2-3.

Figure 14 (a) depicts the original foot MRI image and Figure 14 (b) depicts the reconstructed image obtained using Basic Square method that is L_1 norm minimization. Similarly, the original foot CT-Scan image and recovered image using L_1 norm minimization is depicted in Figure 15 (a) and Figure 15 (b) respectively. This is further validated after analysing the different performance assessment parameters for L_1 reconstruction algorithm obtained in Table 4.

Analysis of performance metrics like RMSE, PSNR and SSIM is done in Table 4 for different medical image samples recovered using L_1 recovery algorithm. L_1 recovery algorithm gives high value of PSNR and lower RMSE value as compared to the previously evaluated recovery methods; L_2 and OMP recovery techniques. Higher value of SSIM is obtained from the L_1 recovery technique out of three evaluated techniques. It is estimated that recovered image is much similar to the original image when L_1 recovery method is used and higher values of performance parameters are also obtained for L_1 reconstruction technique.

Figure 14. (a) Original image of foot MRI-Scan, (b) reconstructed image obtained from Basic Pursuit (L_1) and (c) histogram of original image and (d) histogram of reconstructed image

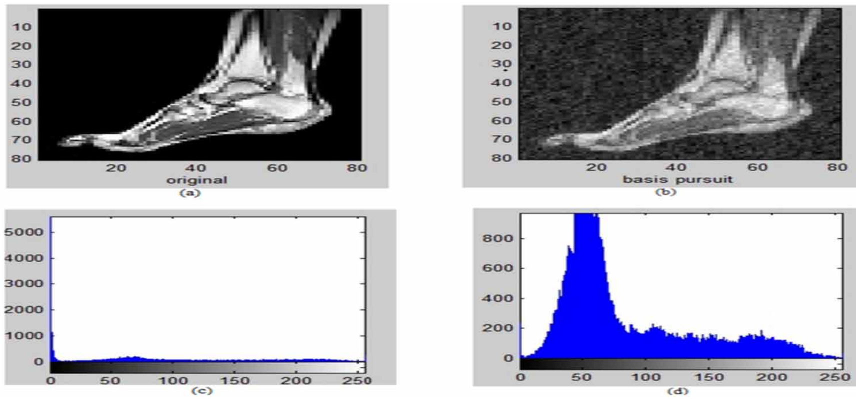

Figure 15. (a) Original image of foot CT-Scan, (b) reconstructed image obtained from Basic Pursuit (L_1) and (c) histogram of original image and (d) histogram of reconstructed image

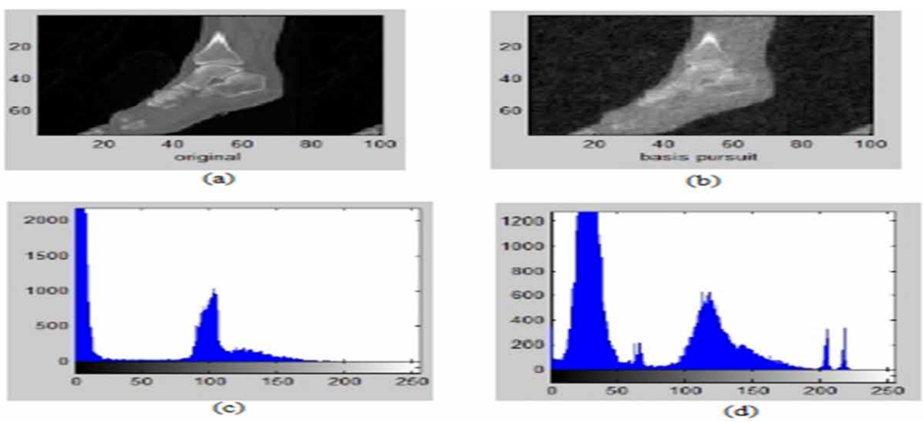

Table 4. Different performance parameters obtained for L_1 recovery algorithm

Image Samples	RMSE	PSNR (dB)	SSIM
Img1_MR	23.38	20.06	0.69
Img2_MR	19.61	21.87	0.65
Img3_MR	22.34	20.22	0.71
Img4_MR	20.15	21.17	0.72
Img5_MR	18.62	22.91	0.66
Img1_CT	21.34	20.05	0.61
Img2_CT	11.83	25.92	0.64
Img3_CT	9.03	28.87	0.60
Img4_CT	22.50	19.93	0.61
Img5_CT	36.31	17.49	0.64

Compression Ratio (CR) is calculated when CS is applied on image samples and it is obtained by taking the ratio of original image bits to the recovered image bits. There should be a trade-off between CR and image quality of an image. CR should be maintained in such a way that there is no degradation of reconstructed image quality. Space saving and CR for different compressed MRI images are graphically represented in Figure 16, graphical representation for different CT images is shown in Figure 17.

Effect of Measurement Samples on Different Image Samples

Foot MRI testing and recovery at varying measurement samples (m) employing L_1, L_2 and OMP reconstruction techniques is shown in Figure 18 to Figure 20 and it shows significant change in recovered images at different m samples. Previously, the effect of m measurement samples are verified for 1D signal and here in this section effect of varying m samples are verified for 2D signal (image). For an image, value of m measurement samples is considered less than the total number of pixels in an image.

Figure 16. Compression ratio and space saving from Compressive Sensing technique for different MRI images

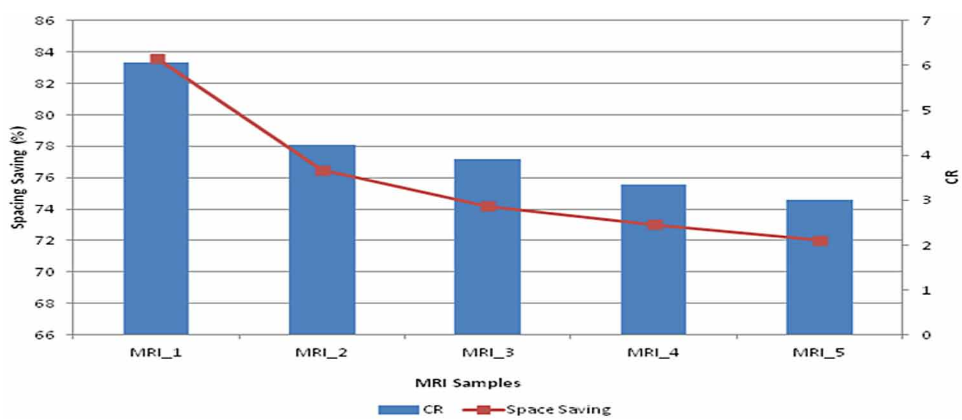

Figure 17. Compression ratio and space saving from Compressive Sensing technique for different CT images

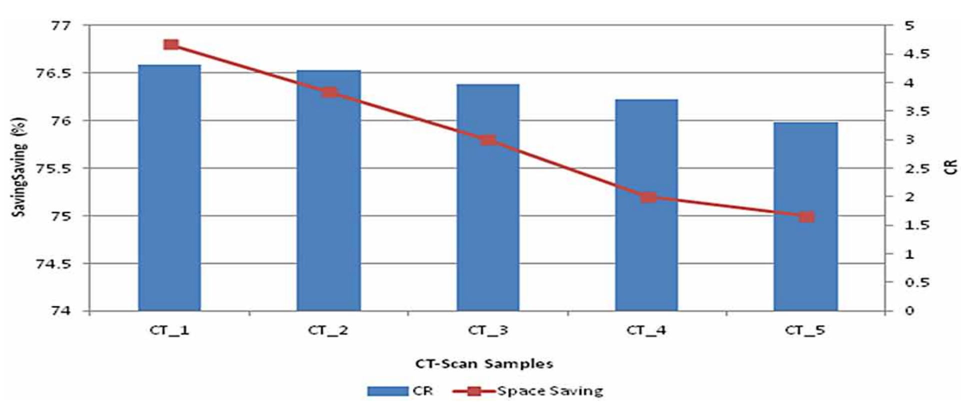

For e.g., for an image having dimension 80×80, n number of samples are 6400 and m can be any value less than 6400. To verify the effect of varying m measurement samples for better image recovery, m is considered 1000, 2000 and 4000 for an image of resolution 80×80. Only single brain MRI image analysis for varying measurement samples is shown in the following figures however the analysis is done for different image modalities.

It is clear from the above figures from Figure 20 to Figure 22 that quality of recovered image is improved when number of m samples is increased. In Figure 20, number of m samples is less i.e., *1000* so the recovered images from all three recovery techniques are of low quality. When number of samples (m) is increased from *1000* to *4000* as shown in Figure 21 and Figure 22, quality of recovered image

Figure 18. (a) Original MRI image of foot, reconstructed image using (b) Least Square (L_2), (c) Matching Pursuit (OMP) and (d) Basic Pursuit (L_1) reconstruction methods at measurement samples m=1000 samples over original image samples n=6400

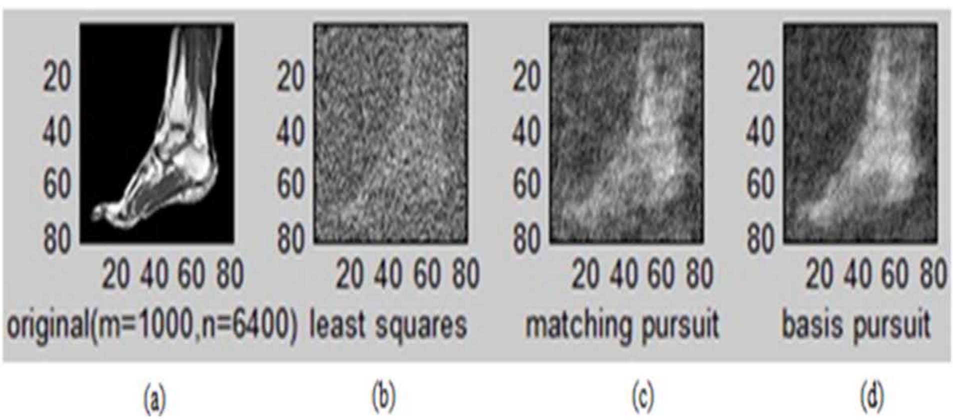

Figure 19. (a) Original MRI image of foot, reconstructed image using (b) Least Square (L_2), (c) Matching Pursuit (OMP) and (d) Basic Pursuit (L_1)reconstruction methods at measurement samples m=2000 samples over original image samples n=6400

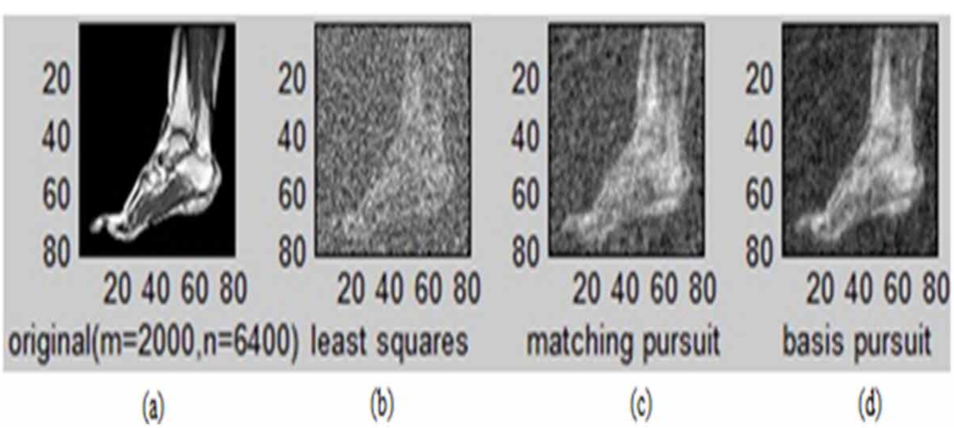

Figure 20. (a) Original MRI image of foot, reconstructed image using (b) Least Square (L_2), (c) Matching Pursuit (OMP) and (d) Basic Pursuit (L_1) reconstruction methods at measurement samples m=4000 samples over original image samples n=6400.

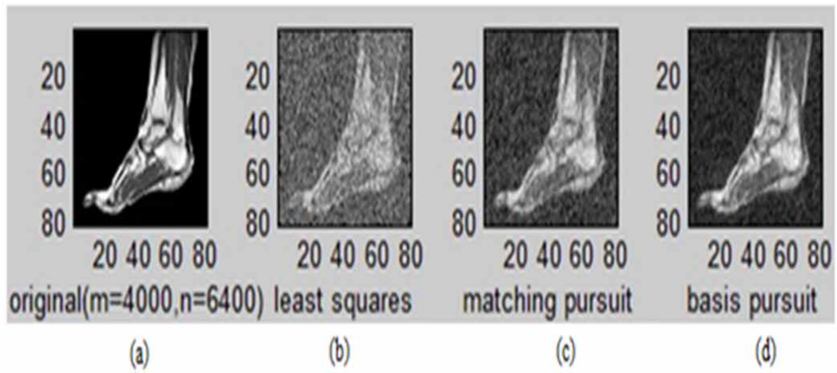

is improved. So number of samples (*m*) should be adjusted in such a way that there is balance between quality of recovered image *(PSNR)* and compression performance *(CR).*

The effect of performance metrics PSNR and RMSE is seen with variation in measurement samples. At different measurement samples for MRI of brain, PSNR and RMSE are calculated. For all three recovery algorithms, PSNR is obtained at *m* = 1000, 2000 and then at 4000 when total number of samples (*n*) are 6400 (resolution of foot MRI) and *m* can be any number less than *n*. It is estimated that value of PSNR increase when number of measurement samples increases. Hence *m* should be selected such that the recovered image is of high quality with higher value of CR.

When *m =1000*, it is seen that PSNR value is around 9 to 15 dB and when it is varied from 1000 to 4000 then PSNR value increases with increase in *m.* Change in PSNR value for recovered images obtained using L_1, L_2 and OMP algorithms is shown in Figure 21 for varying number of samples from 1000 to 4000.

RMSE should be minimized to obtain better image quality. At *m*=1000, higher value of RMSE is obtained for all three recovery algorithms and when *m* is increased from 1000 to 4000, RMSE starts

Figure 21. Measurement samples v/s PSNR for brain MRI

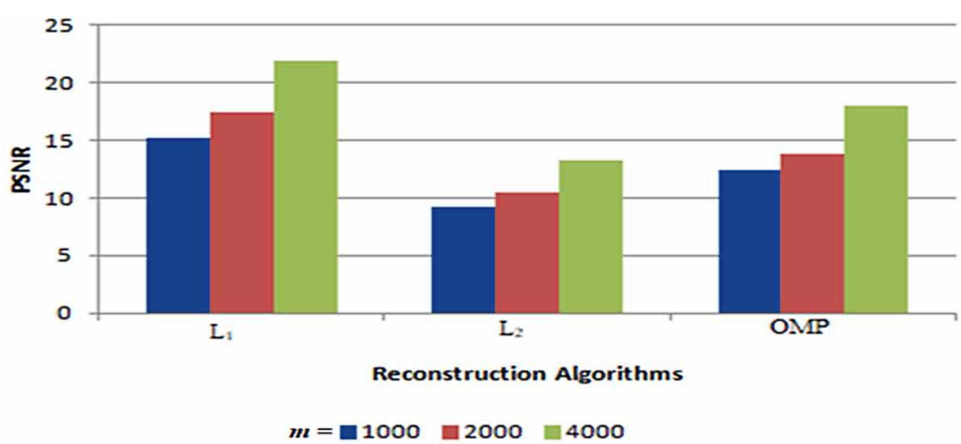

Figure 22. Measurement samples v/s RMSE for brain MRI

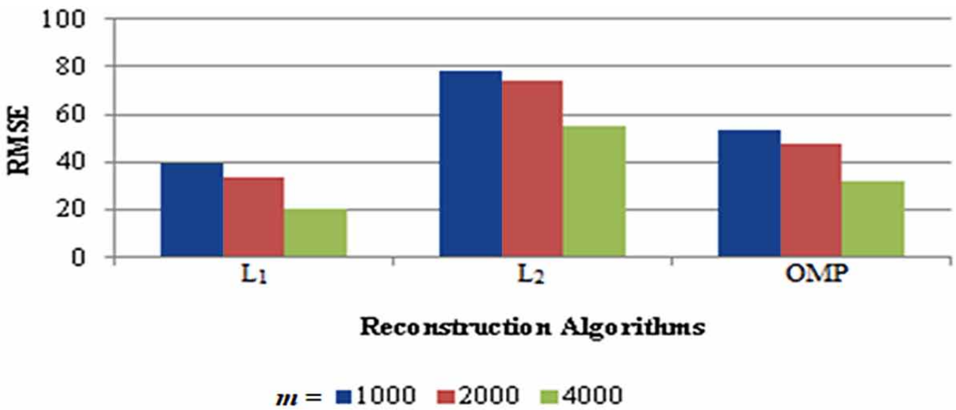

decreasing. RMSE values obtained for L_1, L_2 and OMP recovered images are graphically shown in Figure 22. Out of these three recovery algorithms, the image recovered using L_1 technique provides minimum RMSE value which indicates that the quality of image recovered by L_1 is better than other two algorithms.

CONCLUSION

CS performance is estimate for 1D signal and different medical image samples of MRI and CT- Scan. It is observed that the value of samples should be taken in such a way that there is appropriate balance between the recovered image quality and sampling rate. Quality metrics are obtained for L_1, L_2 and OMP algorithms for different image samples and it is estimated that L_1 technique is better than other reconstruction algorithms in terms of PSNR, RMSE, SSIM and CR. Perfect image recovery is possible by L_1 technique as it resembles more to the original image in comparison to L_2 and OMP reconstruction methods. It is concluded that all quality metrics are better obtained by L_1 and this is the best recovery technique among other implemented algorithms. Thus for a CS based system, L_1 recovery algorithm is considered as a good compression technique that enables a compromise between compression performance and recovered image quality. It is also concluded that the algorithm performance is also altered by the number of measurement samples taken for reconstruction. Value of PSNR increases with increase in number of measurement samples and RMSE value decreases. CS based recovery algorithms can also be implemented for various other medical samples of varying resolution and modality to obtain improved quality image by achieving higher value of PSNR. Compressed sensing concept can also be applied to video signals and the future scope in this field will focus on attaining maximum value of CR along with accurate reconstruction.

REFERENCES

Baig, M. Y., Lai, E. M., & Punchihewa, A. (2012). Compressive Video Coding: A Review of the State-Of-The-Art. In Video Compression. InTech.

Baraniuk, R. G. (2007). Compressive sensing. *IEEE Signal Processing Magazine*, *24*(4), 118–121. doi:10.1109/MSP.2007.4286571

Bhardwaj, C., Ji, U., & Sood, M. (2017). Implementation and Performance Assessment of Compressed Sensing for Images and Video Signals. *Journal of Global Pharma Technology*, *6*(9), 123–133.

Bhatt, M. U., & Bamniya, K. (2015). *Medical Image Compression and Reconstruction Using Compressive Sensing*. Academic Press.

Bilal, M., Ahmed, A. H., Shah, J. A., Kadir, K., & Ayob, M. Z. (2017, September). Comparison of L 1-norm surrogate functions used for the recovery of MR images. In *Engineering Technology and Technopreneurship (ICE2T), 2017 International Conference on* (pp. 1-4). IEEE.

Blumensath, T., & Davies, M. E. (2009). Iterative hard thresholding for compressed sensing. *Applied and Computational Harmonic Analysis*, *27*(3), 265–274. doi:10.1016/j.acha.2009.04.002

Candes, E., & Romberg, J. (2007). Sparsity and incoherence in compressive sampling. *Inverse Problems*, *23*(3), 969–985. doi:10.1088/0266-5611/23/3/008

Candès, E. J., Romberg, J., & Tao, T. (2006). Robust uncertainty principles: Exact signal reconstruction from highly incomplete frequency information. *IEEE Transactions on Information Theory*, *52*(2), 489–509. doi:10.1109/TIT.2005.862083

Candes, E. J., & Tao, T. (2006). Near-optimal signal recovery from random projections: Universal encoding strategies? *IEEE Transactions on Information Theory*, *52*(12), 5406–5425. doi:10.1109/TIT.2006.885507

Candès, E. J., & Wakin, M. B. (2008). An introduction to compressive sampling. *IEEE Signal Processing Magazine*, *25*(2), 21–30. doi:10.1109/MSP.2007.914731

Chang, C. H., & Ji, J. (2010, August). Improved compressed sensing MRI with multi-channel data using reweighted l 1 minimization. In *Engineering in Medicine and Biology Society (EMBC), 2010 Annual International Conference of the IEEE* (pp. 875-878). IEEE.

Donoho, D. L. (2006). Compressed sensing. *IEEE Transactions on Information Theory*, *52*(4), 1289–1306. doi:10.1109/TIT.2006.871582

Eldar, Y. C., Kuppinger, P., & Bolcskei, H. (2010). Block-sparse signals: Uncertainty relations and efficient recovery. *IEEE Transactions on Signal Processing*, *58*(6), 3042–3054. doi:10.1109/TSP.2010.2044837

Foucart, S., & Rauhut, H. (2013). *A mathematical introduction to compressive sensing*. Basel: Birkhäuser.

Hemalatha, R., Radha, S., Raghuvarman, N., Soumya, B., & Vivekanandan, B. (2013). Energy Efficient Image Transmission over Bandwidth Scarce WSN using Compressed Sensing. *International Conference on IT and Intelligent Systems,* 57-61.

Ji, U., Bhardwaj, C., & Sood, M. (2017). Effectiveness of Reconstruction Methods in Compressive Sensing for Biomedical Images. *Journal of Global Pharma Technology*, *6*(9), 134–143.

Jing, C., Wang, Y., & Hanxiao, W. (2012). A Coded Aperture Compressive Imaging Array and Its Visual Detection and Tracking Algorithms for Surveillance Systems. *Sensors (Basel)*, *12*(11), 14397–14415. doi:10.3390121114397 PMID:23202167

Lakshminarayana, M., & Sarvagya, M. (2016). Algorithm to balance compression and signal quality using novel compressive sensing in medical images. In *Software Engineering Perspectives and Application in Intelligent Systems* (pp. 317–327). Cham: Springer. doi:10.1007/978-3-319-33622-0_29

Liang, D., & Ying, L. (2010, August). Compressed-sensing dynamic MR imaging with partially known support. In *Engineering in Medicine and Biology Society (EMBC), 2010 Annual International Conference of the IEEE* (pp. 2829-2832). IEEE. 10.1109/IEMBS.2010.5626077

Liu, D. D., Liang, D., Liu, X., & Zhang, Y. T. (2012, August). Under-sampling trajectory design for compressed sensing MRI. In *Engineering in Medicine and Biology Society (EMBC), 2012 Annual International Conference of the IEEE* (pp. 73-76). IEEE.

Liu, Y., De Vos, M., Gligorijevic, I., Matic, V., Li, Y., & Van Huffel, S. (2013). Multi-structural signal recovery for biomedical compressive sensing. *IEEE Transactions on Biomedical Engineering*, *60*(10), 2794–2805. doi:10.1109/TBME.2013.2264772 PMID:23715599

Madhukumar, N., & Baiju, P. S. (2015). Contourlet Transform Based MRI Image Compression using Compressed Sensing. *International Journal of Advanced Research in Electrical, Electronics and Instrumentation Engineering, 4*(7), 6434-6440.

Majumdar, A., Ward, R. K., & Aboulnasr, T. (2012). Compressed sensing based real-time dynamic MRI reconstruction. *IEEE Transactions on Medical Imaging*, *31*(12), 2253–2266. doi:10.1109/TMI.2012.2215921 PMID:22949054

ME, M. S. S., Vijayakuymar, V. R., & Anuja, M. R. (2012). A survey on various compression methods for medical images. *International Journal of Intelligent Systems and Applications, 4*(3), 13.

Nagesh, P., & Baoxin, L. (2009). A Compressive Sensing Approach for Expression-Invariant Face Recognition. *IEEE Conference on Computer Vision and Pattern Recognition*, 1518-1525. 10.1109/CVPR.2009.5206657

Nahar, P. C., & Kolte, M. T. (2014). An introduction to compressive sensing and its applications. *Int J Sci Res Publ, 4*(6).

Park, J. Y., & Wakin, M. B. (2009, May). A multiscale framework for compressive sensing of video. In *Picture Coding Symposium, 2009. PCS 2009* (pp. 1-4). IEEE. 10.1109/PCS.2009.5167440

Qu, X., Cuo, X., Guo, D., Hu, C., & Chen, Z. (2010). Compress sensing MRI with combined sparisifying transforms and smoothed l0 norm minimization. *International Conference of IEEE*, 626-629.

Ravishankar, S., & Bresler, Y. (2011, August). Adaptive sampling design for compressed sensing MRI. In *Engineering in Medicine and Biology Society, EMBC, 2011 Annual International Conference of the IEEE* (pp. 3751-3755). IEEE. 10.1109/IEMBS.2011.6090639

Satyan, S. (2013). *The Use of Compressive Sensing in Video* (Doctoral dissertation).

Sen, P., & Darabi, S. (2011). Compressive Rendering: A Rendering Application of Compressed Sensing. *IEEE Transactions on Visualization and Computer Graphics*, *17*(4), 487–499. doi:10.1109/TVCG.2010.46 PMID:21311092

Sevak, M. M., Thakkar, F. N., Kher, R. K., & Modi, C. K. (2012, May). CT image compression using compressive sensing and wavelet transform. In *Communication Systems and Network Technologies (CSNT), 2012 International Conference on* (pp. 138-142). IEEE. 10.1109/CSNT.2012.39

Shiqian, M., Wotao, Y., Yin, Z., & Chakraborty, A. (2008). An Efficient Algorithm for Compressed MR Imaging using Total Variation and Wavelets. *IEEE Conference on Computer Vision and Pattern Recognition*, 1-8. 10.1109/CVPR.2008.4587391

Shrividya, G., & Bharathi, S. H. (2018, February). A study of Optimum Sampling Pattern for Reconstruction of MR Images using Compressive Sensing. In *2018 Second International Conference on Advances in Electronics, Computers and Communications* (pp. 1-6). IEEE. 10.1109/ICAECC.2018.8479422

Tran, T. D., Duc, T. T., & Bui, T. T. (2010, November). Combination compress sensing and digital wireless transmission for the MRI signal. In *Micro-NanoMechatronics and Human Science (MHS), 2010 International Symposium* (pp. 273-276). IEEE.

Tremoulheac, B., Dikaios, N., Atkinson, D., & Arridge, S. R. (2014). Dynamic MR Image Reconstruction–Separation From Undersampled (k, t)-Space via Low-Rank Plus Sparse Prior. *IEEE Transactions on Medical Imaging*, *33*(8), 1689–1701. doi:10.1109/TMI.2014.2321190 PMID:24802294

Tropp, J. A. (2004). Greed is good: Algorithmic results for sparse approximation. *IEEE Transactions on Information Theory*, *50*(10), 2231–2242. doi:10.1109/TIT.2004.834793

Tropp, J. A., Gilbert, A. C., & Strauss, M. J. (2006). Algorithms for simultaneous sparse approximation. Part I: Greedy pursuit. *Signal Processing*, *86*(3), 572–588. doi:10.1016/j.sigpro.2005.05.030

Wang, G., Bresler, Y., & Ntziachristos, V. (2011). Guest editorial compressive sensing for biomedical imaging. *IEEE Transactions on Medical Imaging*, *30*(5), 1013–1016. doi:10.1109/TMI.2011.2145070 PMID:21692237

Wiegand, T., Sullivan, G. J., Bjontegaard, G., & Luthra, A. (2003). Overview of the H. 264/AVC video coding standard. *IEEE Transactions on Circuits and Systems for Video Technology*, *13*(7), 560–576. doi:10.1109/TCSVT.2003.815165

Wright, J., Yang, A. Y., Ganesh, A., Sastry, S. S., & Ma, Y. (2009). Robust Face Recognition via Sparse Representation. *IEEE Transactions on Pattern Analysis and Machine Intelligence*, *31*(2), 210–227. doi:10.1109/TPAMI.2008.79 PMID:19110489

Xie, S., Guan, C., Huang, W., & Lu, Z. (2015). Frame-based compressive sensing MR image reconstruction with balanced regularization. In *Engineering in Medicine and Biology Society (EMBC), 2015 37th Annual International Conference* (pp. 7031-7034). IEEE.

Yipeng, L., De, V. M., Gligorijevic, I., Matic, V., & Li, Y. (2013). Multi-Structural Signal Recovery for Biomedical Compressive Sensing. *IEEE Transactions on Biomedical Engineering*, *60*(10), 2794–2805. doi:10.1109/TBME.2013.2264772 PMID:23715599

Zhang, Q., Zhang, J., & Sei-ichiro, K. (2016). Adaptive sampling and wavelet tree based compressive sensing for MRI reconstruction. In *Image Processing (ICIP), 2016 IEEE International Conference*, (pp. 2524-2528). IEEE.

Zhang, X., & Wen, J. (2012, September). Compressive video sensing using non-linear mapping. In *Image Processing (ICIP), 2012 19th IEEE International Conference on* (pp. 885-888). IEEE. 10.1109/ICIP.2012.6467002

Zhang, X., Wen, J., Han, Y., & Villasenor, J. (2011, February). An improved compressive sensing reconstruction algorithm using linear/non-linear mapping. In *Information Theory and Applications Workshop (ITA)*, 2011 (pp. 1-7). IEEE. 10.1109/ITA.2011.5743577

Zhao, C., Ma, S., Zhang, J., Xiong, R., & Gao, W. (2017). Video compressive sensing reconstruction via reweighted residual sparsity. *IEEE Transactions on Circuits and Systems for Video Technology*, *27*(6), 1182–1195. doi:10.1109/TCSVT.2016.2527181